Soft Matter

ARTICLE

Nanomechanics of Layer-by-Layer Polyelectrolyte Complexes: A Manifestation of Ionic Cross-links and Fixed Charges

Biao Han,[a] Daphney R. Chery,[a] Jie Yin,[b] X. Lucas Lu,[c] Daeyeon Lee,[d] Lin Han[a,]*

Supporting Information – Appendix

A1. Technical advances in polymer film thickness measurement

The *z*-motor assisted AFM thickness measurement, or the "*z*-motor method", developed in this study offers a novel approach to quantify the thickness, H, of highly swollen polymer films (H > 10 μm) that are transparent in fluid (Fig. 2a). Current practices of film thickness measurement mainly include ellipsometry,[85] light or contact-based profilometry,[86-88] and AFM imaging after selective film removal.[57] In ellipsometry, one of the most prevailing method, H is calculated by the phase and amplitude shift of a polarized elliptical light resulting from the refractive index contrasts between the film and substrate.[89] Ellipsometry is highly accurate and easy to operate for both dry and wet films. Its accuracy is, however, largely reduced for films at highly swollen, transparent state, where the film refractive index is similar to its fluid environment. Other light-based profilometry techniques, such as dual polarization interferometer,[86] and laser triangulation sensor,[87] adopt similar principles of light/laser reflection or refraction contrast, and thus, also have limited applications for transparent films. In contact-based profilometry, a spherical stylus (~ 10 μm in diameter) is programmed to scan across partially-removed film surface at a tare force ~ 10 μN, and H is directly measured by tracking the stylus movement.[88] It is often used to quantify H of dry films, where the deformation or wear induced by the tare force is negligible.[90] Its application in the wet state is much limited, as this μN-level tare force can result in marked film deformation and wear. In comparison, AFM-based imaging measures H in a similar fashion by programming a probe tip scanning across a partially removed film surface,[57] albeit at a much smaller tare force (~ 1 nN or less). Since the AFM height sensor has a resolution as high as 0.1 nm, AFM imaging is likely the most accurate and direct way to quantify film thickness in fluid (Fig. 2a). However, this method is restricted by the upper limit of the *z*-piezo displacement range, normally ~ 10 μm.[58]

In the "*z*-motor method" developed here, thickness measurement relies on the AFM *z*-step motor. The step motor has an upper limit of displacement ≈ 10 cm,[58] which far exceeds the thickness range of all polymer films. It is thus applicable to directly assess the thickness of all films at both dry and wet states. However, this method has a much lower spatial resolution (≈ 0.1 μm)[58] compared with the AFM piezo-based imaging and other methods. For example, for the same PAH/PAA film at pH 3.0, 0.1M, H measured by *z*-motor method yields similar average but much larger standard error than the value measured by contact mode AFM imaging (Fig. 2c). In this study, for PAH/PAA, we applied contact mode AFM imaging when $H \leq 10$ μm, and the *z*-motor method when $H \geq 10$ μm (methods I and II in Fig. 2, respectively). At the highly swollen states, the *z*-motor method yields a systematic error of ≈ 1% or less, negligible in comparison to the film heterogeneity and variations across different states.

A2. Technical considerations in nanomechanical studies of highly rate-dependent polymer networks

Results from nanoindentation experiments suggest that it is critical to maintain a constant indentation depth rate, $\upsilon_D = \partial D/\partial t$, when quantifying the mechanical properties of highly rate-dependent polymer networks via AFM. In AFM-nanoindentation, a silicon or silicon nitride cantilever end-attached with a probe tip is driven to indent the sample by the *z*-piezo, whereby the indentation force, F, linearly scales with the upward bending of the cantilever, b_c. During the indentation, the *z*-piezo displacement, d_z, represents the sum of indentation depth, D, and cantilever bending, b_c (**Fig. S1**). Correspondingly, the *z*-piezo ramp velocity, $\upsilon_z = \partial d_z/\partial t$, is the sum of indentation rate, υ_D, and the cantilever bending rate, $\upsilon_c = \partial b_c/\partial t$.

$$d_z = D + b_c,$$
$$\upsilon_z = \upsilon_D + \upsilon_c.$$

During conventional nanoindentation, υ_z is maintained at constant, and υ_D decreases as υ_c increases due to the nonlinear increase in force with depth (**Fig. S2**a). When the testing materials are stiff compared to the cantilever spring constant ($k \approx 5.4$ N/m here), at a constant υ_z, υ_c is comparable to υ_D. The deviation in $\upsilon_D = \upsilon_z - \upsilon_c$ from υ_z is thus substantial (Fig. S2a). Furthermore, when the mechanical properties of testing materials are highly rate-dependent, this deviation can result in major systematic errors in the measured modulus. One example is PAH/PAA at pH 5.5, 0.01M, where E_0 is relatively high and viscoelasticity dominates. At this state, E_0 is 64.9 ± 0.3% lower when measured at constant υ_z = 5 μm/s via conventional AFM-

[a] *School of Biomedical Engineering, Science, and Health Systems, Drexel University, Philadelphia, PA 19104, United States*
[b] *Department of Mechanical Engineering, Temple University, Philadelphia, PA 19122, United States*
[c] *Department of Mechanical Engineering, University of Delaware, Newark, DE 19716, United States*
[d] *Department of Chemical and Biomolecular Engineering, University of Pennsylvania, Philadelphia, PA 19104, United States*

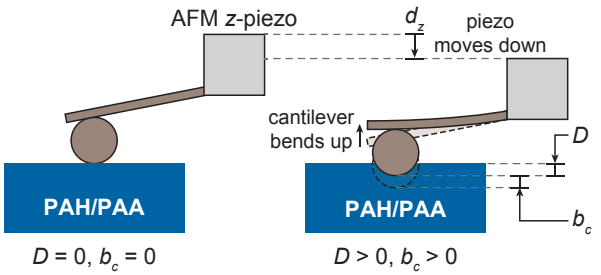

Fig. S1 Schematic of the relationships between AFM *z*-piezo downward displacement, d_z, indentation depth, D, and cantilever upward bending, b_c, during nanoindentation shows that $D = d_z - b_c$. velocity, $\upsilon_z = \partial d_z/\partial t$, is the sum of indentation rate, υ_D, and the cantilever bending rate, $\upsilon_c = \partial b_c/\partial t$.

nanoindentation (equivalent υ_D = 1.43 ± 0.08 μm/s) than E_0 measured at constant υ_D = 5 μm/s (Fig. S2b,c). In contrast, the errors in rate are attenuated when indenting on softer networks, where υ_c is much smaller than υ_D. In addition, when the materials are more elastic, this deviation in rate has even less impacts on the modulus. One example for this scenario is PAH/PAA at pH 2.0, 0.01M, where E_0 is approximately hundred-fold lower (Fig. 4a) but less rate-dependent (Fig. 6). At the same υ_z = 5 μm/s, given a much smaller υ_c, the deviation in υ_D is very minor (Fig. S2d). In addition, as PAH/PAA is less rate-dependent at pH 2.0, 0.01M (Fig. 5b), the impacts of deviation in υ_D are negligible on the indentation *F-D* curves (Fig. S2e) and E_0 (Fig. S2f). Therefore, if the modulus changes of PAH/PAA at pH 5.5 versus 2.0 were studied via conventional AFM-nanoindentation at constant υ_z, due to the differences in the deviation of υ_D and its impacts on E_0, the pH-responsiveness of E_0 is underestimated by a factor of 2.7 ± 0.1 ×.

In addition, the force relaxation experiments underline the importance of maintaining a constant indentation depth, D, when studying the time-dependent mechanics of highly viscoelastic, ionic networks (**Fig. S3**). During conventional AFM-based ramp-and-hold relaxation test, the *z*-piezo displacement, d_z, instead of the indentation depth, D, is kept constant during the holding period. During relaxation, indentation force, F, and thus, cantilever bending, b_c, decreases due to the reduction in modulus. At a constant d_z, $D = d_z - b_c$ (Fig. S1) thus increases simultaneously and results in a combination of force relaxation and creep (Fig. S3a). For example, for PAH/PAA at pH 5.5, 0.01M, measuring relaxation at constant d_z results in continuous change of D (curve B in Fig. S3a). Since force relaxation and creep takes place simultaneously, the viscoelastic behaviors of ionic networks are very different from the single mode of force relaxation. As a result, even after the variations in D are taken into account, the temporal modulus, $E(t)$, exhibits a completely different pattern from that measured at constant D (Fig. S3b). This complication leads to a 14.9 ± 1.0 × higher ratio of E_∞/E_0 (Fig. S3c), and thus, drastically overestimates the weight of elastic component in the overall modulus. In contrast, when the networks are more elastic, such as PAH/PAA at pH 2.0, 0.01M, the cross-talk of creep due to variations in D (Fig. S3d) has much less impacts in the relaxation pattern (Fig. S3e). Values of E_∞ are not significantly affected if variations in D are taken into account (Fig. S3f). Taken together, for highly viscoelastic ionic networks such as PAH/PAA, conventional AFM ramp-and-hold relaxation test at constant d_z will largely overestimate the elastic component and obscure the intrinsic relaxation behaviors.

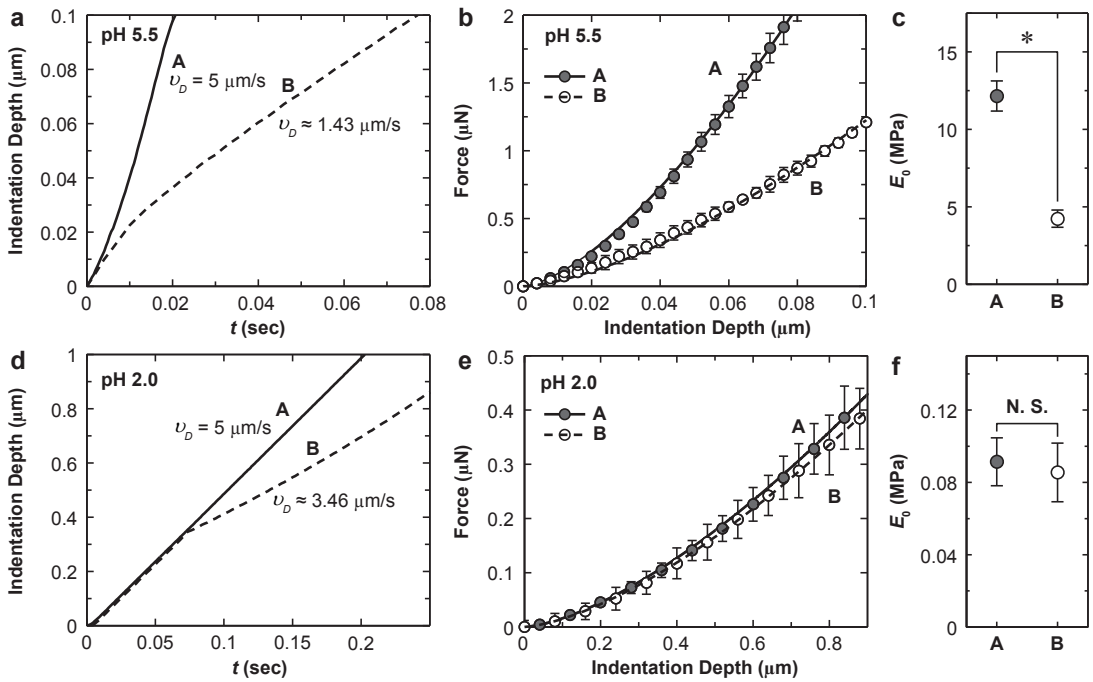

Fig. S2 Comparison of AFM-nanoindentation under constant indentation-depth rate control (mode A) versus constant *z*-piezo displacement open-loop control (mode B), demonstrated by the measurement of PAH/PAA at 0.01M IS, (a-c) pH 5.5 and (d-f) pH 2.0, respectively. (a,d) Typical indentation depth versus time curves during nanoindentation, (b, e) typical indentation force versus depth (*F-D*) curves measured by the two modes (mean ± STD of ≥ 10 positions for each curve), and (c, f) comparison of indentation modulus, E_0, by the two modes (mean ± SEM, $n \geq 15$, *: $p < 0.0001$ via Mann-Whitney U test for pH 5.5 in panel c, and $p > 0.05$ at pH 2.0 in panel f).

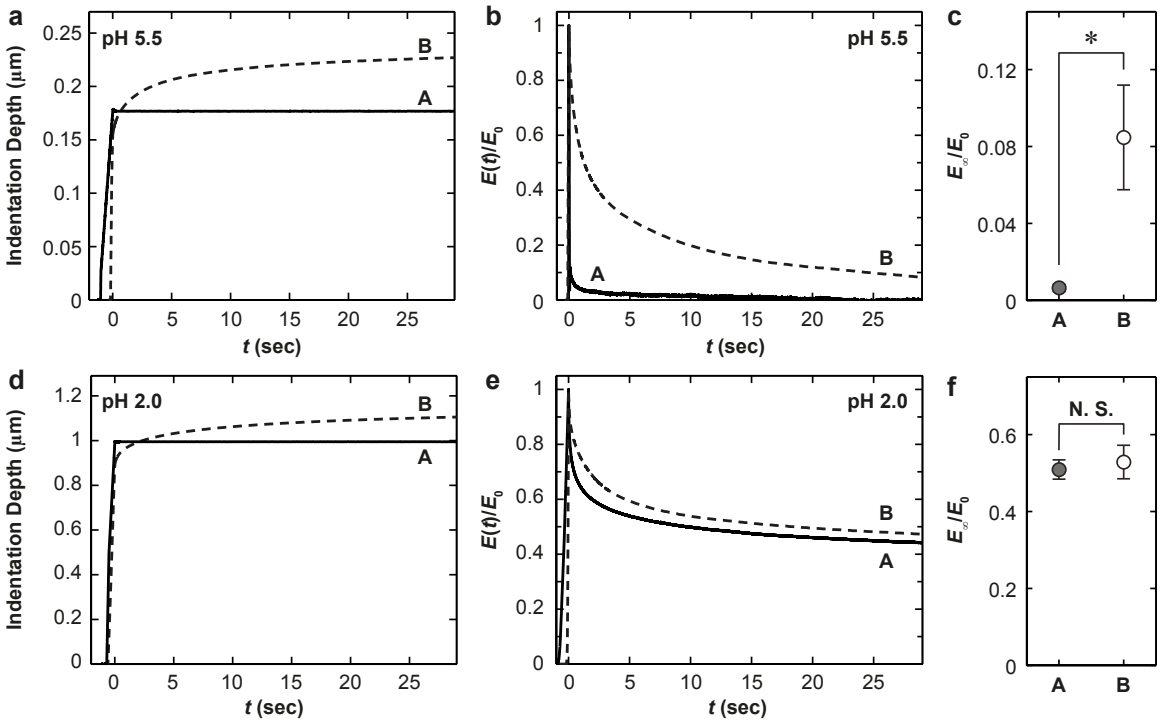

Fig. S3 Comparison of AFM ramp-and-hold force relaxation under constant indentation depth control (mode A) versus constant *z*-piezo location open-loop control (mode B), demonstrated by the measurement of PAH/PAA at 0.01M IS, (a-c) pH 5.5 and (d-f) pH 2.0, respectively. (a, d) Typical indentation depth versus time curves during the relaxation experiment, (b, e) typical time-domain relaxation of modulus, $E(t)$, normalized by the initial modulus, E_0, and (c, f) comparison of degree of relaxation, E_∞/E_0, measured by two modes (mean ± SEM, $n \geq 15$, *: $p < 0.001$ via Mann-Whitney U test for pH 5.5 in panel c, and $p > 0.05$ at pH 2.0 in panel f).